

Focal posterior cingulate atrophy in incipient Alzheimer's disease

George Pengas^a, John R. Hodges^c, Peter Watson^b, Peter J. Nestor^{a,*}

^a University of Cambridge, Neurology Unit, Addenbrooke's Hospital, Cambridge CB2 0QQ, UK

^b MRC Cognition and Brain Sciences Unit, 15 Chaucer Road, Cambridge CB2 2EF, UK

^c Prince of Wales Medical Research Institute, Barker Street, Randwick, NSW 2031, Australia

Received 28 September 2007; received in revised form 14 March 2008; accepted 22 March 2008

Available online 2 May 2008

Abstract

Severe posterior cingulate cortex hypometabolism is a feature of incipient, sporadic Alzheimer's disease (AD). The aim was to test the hypothesis that this region is focally atrophic in very early disease by studying AD patients at the mild cognitive impairment (MCI) stage, and, if so, to determine whether the amount of atrophy was comparable to that of the hippocampus. Twenty-four patients meeting criteria for amnesic MCI, who all subsequently progressed to fulfil AD criteria, and 28 age-matched controls, were imaged with volumetric MRI. Four regions of interest were manually traced in each hemisphere: two posterior cingulate regions (BA 23 and BA 29/30), the hippocampus (as a positive control) and the anterior cingulate (as a negative control). BA 23 and BA 29/30 were both significantly atrophic and this atrophy was comparable to that found in the hippocampus, in the absence of anterior cingulate cortex (ACC) atrophy. Contrary to previous reports, there was no evidence that posterior cingulate atrophy is specifically associated with early-onset AD. The results indicate that posterior cingulate cortex atrophy is present from the earliest clinical stage of sporadic AD and that this region is as vulnerable to neurodegeneration as the hippocampus. © 2008 Elsevier Inc. All rights reserved.

Keywords: Mild cognitive impairment; Alzheimer's disease; Posterior cingulate; Manual volumetry

1. Introduction

A large body of structural imaging research in Alzheimer's disease (AD) has been devoted to the mesial temporal lobe (MTL). There is good reason for this—focal hippocampal lesions cause episodic memory impairment (Zola-Morgan et al., 1986), episodic memory impairment is the earliest clinical deficit in AD and the hippocampus and adjacent entorhinal cortex are the sites of earliest tau deposition in AD (Braak and Braak, 1991). Numerous volumetric magnetic resonance imaging (MRI) studies have confirmed that the hippocampus is atrophic in AD cohorts (e.g. Jack et al., 1997a; Wahlund et al., 2000; Chan et al., 2001; Galton et al., 2001) and this is also true of groups with incipient disease (i.e. when scanned at the amnesic mild cognitive impairment (MCI) stage) (Jack et al., 1999).

(18)F-fluorodeoxyglucose positron emission tomography (FDG-PET) imaging in AD has highlighted a different lesion. The advent of voxel-based image analysis led to the discovery that the earliest hypometabolic region in AD is the posterior cingulate cortex (Minoshima et al., 1997). This FDG-PET lesion is also evident at the MCI stage of AD (Nestor et al., 2003). Mesial temporal structures are also hypometabolic in incipient AD (De Santi et al., 2001; Nestor et al., 2003), however when the metabolic rate of the MTL and posterior cingulate was calculated in the same cohort, it was notable that the posterior cingulate lesion was considerably more significant (Nestor et al., 2003).

Posterior cingulate hypometabolism in incipient AD was initially interpreted as representing physiological deafferentation from the MTL (Minoshima et al., 1997; Nestor et al., 2003). However, in semantic dementia (SD), a variant of frontotemporal dementia with predominant temporal lobe atrophy, patients were found to have at least as severe MTL atrophy and hypometabolism as that seen in AD, yet did not display posterior cingulate hypometabolism (Nestor et al., 2006). This finding challenged the deafferentation hypothe-

* Corresponding author at: Department of Clinical Neuroscience, Box 83, Addenbrooke's Hospital, Hills Road, Cambridge CB2 2QQ, UK.
Tel.: +44 1223 355294x393; fax: +44 1223 516630.

E-mail address: pjn23@hermes.cam.ac.uk (P.J. Nestor).

sis in AD; the alternative explanation is that rather than being predominantly a physiological phenomenon, focal posterior cingulate hypometabolism in incipient AD is, to a significant degree, a consequence of local, and specific, neurodegeneration. Our aim was to test the hypothesis that this region is focally atrophic in very early disease by studying AD patients at the MCI stage, and, if so, to determine whether the amount of atrophy was comparable to that of the hippocampus.

Voxel-based morphometry (VBM) studies in MCI have produced mixed results, both in terms of posterior cingulate (absent, unilateral or bilateral) as well as hippocampal (unilateral or bilateral) involvement (Karas et al., 2004; Chetelat et al., 2005; Pennanen et al., 2005; Bozzali et al., 2006; Shiino et al., 2006; Whitwell et al., 2007). The reasons for this variability may include methodological differences and subject selection.

Therefore, a manual volumetric approach was adopted. Two posterior cingulate regions – Brodmann area (BA) 29/30 (retrosplenial cortex) and BA 23 – were sampled in an incipient AD cohort (i.e. patients scanned at the amnesic MCI stage but who subsequently declined to AD with longitudinal follow-up). This approach to case selection meant that we could assess atrophy in patients with the earliest form of AD, without diluting our sample with non-AD pathology, as can happen in studies of MCI groups without longitudinal confirmation of AD. The results were contrasted, within subjects, to hippocampal volumes to assess whether the magnitude of any identified atrophy would be comparable. Furthermore, to ensure that posterior cingulate atrophy, if found, was specific (rather than merely reflecting a sampling of general cortical atrophy), the anterior cingulate (BA 24 and 33) was measured as a negative control region (Callen et al., 2001). While other manual volumetric studies have examined the relative amounts of atrophy in subdivisions of the posterior cingulate, with, (Callen et al., 2001; Barnes et al., 2007), and without comparison to the hippocampus (Jones et al., 2006), these were all performed in patients with established AD. To our knowledge, this is the first study that has directly compared the relative atrophy of hippocampal and cingulate structures at the MCI-stage, in patients destined to fulfil probable AD criteria. Finally, some authors have proposed that posterior cingulate degeneration is more marked in early-onset AD, while hippocampal degeneration predominates in late-onset AD (Kemp et al., 2003; Frisoni et al., 2005; Shiino et al., 2006). The effect of age of disease onset on hippocampal and posterior cingulate atrophy was therefore assessed.

2. Methods

2.1. Subjects

Twenty-four subjects who met criteria for amnesic MCI were recruited from the Cambridge longitudinal MCI cohort study (Alladi et al., 2006). These criteria were (1) subjective memory symptoms corroborated by an informant; (2)

Table 1
Demographic data

	Incipient AD	Controls	<i>p</i>
Gender (M:F)	9:15	17:11	NS ($\chi^2 = 2.8$)
Age at imaging (years)	68.6 (6.9)	64.8 (8.6)	NS
Education (years)	12.6 (3.3)	10.8 (1.4)	0.044
MMSE at imaging/30	26.7 (1.4)	29.3 (0.8)	<0.0001
ACE at imaging/100	83.2 (5.1)	94.1 (3.6)	<0.0001

Key: M, male; F, female; MMSE, Mini Mental State Examination; ACE, Addenbrooke's Cognitive Examination; AD, Alzheimer's disease; NS, non-significant (standard deviation).

objective memory impairment (lower than 1.5 standard deviations relative to controls on measures of delayed recall) based on the Rey Auditory Verbal Learning Test; (3) preserved Activities of Daily Living as ascertained by the Cambridge Behavioural Inventory (Nagahama et al., 2006); and (4) no evidence of dementia (based on Mini Mental State Examination (MMSE) (Folstein et al., 1975) score > 24) and Clinical Dementia Rating (Morris, 1993) score of 0.5. The selection criteria were that they had been scanned at baseline, the scans did not have significant motion artefact, and that they subsequently declined with longitudinal follow-up to probable AD, according to NINCDS-ADRDA criteria (McKhann et al., 1984), indicating that their original MCI status represented incipient AD. The mean time between the MRI and fulfilling the diagnostic criteria for probable AD was 1.75 (± 0.9) years.

Twenty-eight age- and sex-matched controls were recruited. All controls were screened to exclude neurological or major psychiatric illness and performed normally on the Addenbrooke's Cognitive Examination (ACE) (Mathuranath et al., 2000). Written informed consent was obtained from all participants. The study was approved by the Local Regional Ethics Committee. See Table 1 for the subjects' demographic details.

2.2. Image acquisition

MR images were acquired with a 1.5 T GE Signa MRI scanner (GE Medical Systems, Milwaukee, WI). Volumetric T1-weighted images were coronally acquired using a spoiled gradient-echo technique (pixel dimension 0.86 mm^2 , slice thickness 1.8 mm). In addition, proton density (PD) and T2-weighted axial dual-echo sequence images were acquired for TIV measurement. All patients were scanned within an average of 2.8 (± 1.9) months from an assessment confirming MCI status.

2.3. Image analysis

All manual measurements were performed with the Analyze version 7.0 software package (Biomedical Imaging Resource, Mayo Clinic, Rochester, MN, USA). The MRI images were first interpolated using the cubic spline function to give cubic voxels (i.e. $0.86 \text{ mm} \times 0.86 \text{ mm} \times 0.86 \text{ mm}$). To

standardise orientation, the acquired images were manually re-aligned (using Analyze) so that the anterior–posterior axis was parallel to the anterior commissure–posterior commissure line and the inter-hemispheric fissure was aligned on the other two axes. The threshold intensity was set to maximise cortical grey:white matter (GM:WM) differentiation without reducing the cortical GM thickness.

2.4. Volumetry

Volumetric analysis was performed by a single observer (GP). All measurements and segmentations were performed while blinded to subject details and the results of any other measurements. The Analyze “seed and expand” (Autotrace) function was used to delineate all ROI along with manual editing as required.

2.4.1. Hippocampus

The landmarks for the delineation of the hippocampus as described by Hasboun et al. (1996) were used, with some modifications, and with the aid of a standard neuroanatomical atlas (Duvernoy, 1999). The hippocampus proper (CA-1 to CA-4), dentate gyrus, alveus, fimbria and subiculum were included. The boundaries were outlined in the coronal plane, at quadruple magnification. The rostral limit of the hippocampal head is known to be difficult to delineate, as the amygdala can be completely overlying it, especially in subjects with little or no atrophy. The axial plane was used to accurately delineate the rostral border of the hippocampal head and the amygdalohippocampal transition area (AHT). The AHT was defined in the axial plane as the narrowest, rostral-most point where the medial part of the hippocampal head merges with the amygdala. The ventral, lateral and superior borders of the hippocampus were delineated as described by Hasboun et al. (1996) (i.e. the GM–WM junction of the entorhinal cortex and subiculum, alveus and temporal horn of the lateral ventricle).

However, we deviated from this protocol (Hasboun et al., 1996) on two occasions. Firstly, the entire subiculum was included, and the border separating the subiculum from the parahippocampal gyrus was defined as the angle formed by the most medial extent of these structures (Watson et al., 1997). Secondly, the posterior limit of the hippocampus was defined as the most rostral coronal slice intersecting the posterior commissure (Jack et al., 1989).

2.4.2. Cingulate gyrus

This gyrus is divided into anterior and posterior cingulate regions. The posterior cingulate can be further subdivided by cytoarchitectonic means into Brodmann areas (BA) 29/30, and BA 23 (Vogt et al., 1995).

The surface features of the human cingulate cortex are variable, including the presence of a deep single cingulate sulcus, or shallower double parallel sulci, either of which may be anatomically discontinuous (Vogt et al., 1995). Furthermore, BA23 and retrosplenial areas do not completely

surround the splenium: immediately ventral to the splenium, area 27 and the parasubiculum take the place of the retrosplenial cortex (Vogt et al., 2001). Finally, as the posterior cingulate cortex curves inferior to the splenium, it also moves laterally away from the midline. This means that coronal and sagittal slices become tangential which, in turn, creates difficulties in delineation of a consistent and reproducible limit between subjects. For these reasons, we adopted sampling protocols for BA 23 and BA 29/30, choosing to measure the more rostral (above the splenium) parts of these areas (see Section 2.4.2.1 below) where the mesial pial surface lies flat against the inter-hemispheric fissure.

2.4.2.1. Posterior cingulate.

2.4.2.1.1. Brodmann areas 29/30 (retrosplenial cortex). Area 29/30 (Vogt et al., 1995) was traced in the sagittal plane, at quadruple magnification. The rostral border was defined as the most rostral coronal slice intersecting the posterior commissure (Fig. 1A) (Jones et al., 2006). The caudal limit was set in the mid-sagittal view as a coronal plane at the caudal-most point of the splenium of the corpus callosum. The inferior border of BA 29/30 is the corpus callosum and the superior border is the cingulum bundle. Area 29/30 does not appear on the medial surface of the cingulate gyrus (Vogt et al., 2001); its medial border was the most medial sagittal slice which did not include BA 23, i.e. in which BA 29/30 was still bordered superiorly by the cingulum bundle. The delineation of BA 29/30 was verified in the coronal plane (Fig. 1B).

2.4.2.1.2. BA 23. BA 23 was traced in the coronal plane, at eight times magnification. The rostral limit was taken to be the most rostral coronal slice intersecting the posterior commissure. The caudal limit was defined as 10 coronal slices (inclusive) caudal to the posterior commissure. The inferior limit was the corpus callosum. Medially, BA 23 was delineated by CSF in the inter-hemispheric fissure and laterally, by the GM–WM border, as well as BA 29/30.

Due to the variability of the cingulate and splenial sulci (Vogt et al., 1995; Jones et al., 2006), a fixed cortical length was used as the superior limit of the cortex in coronal views. The limit was arbitrarily set at 20 mm of cortical ribbon length, measured from the most infero-medial voxel (bordering CSF), along the WM:GM edge of BA 23, but excluding BA 29/30. This was measured using the Border Tool in Analyze. The superior limit of the 20 mm-long cortical ribbon was manually drawn to be perpendicular to the cortical surface (Fig. 1B).

2.4.2.2. Anterior cingulate cortex (ACC). The ACC was traced in the axial plane, at eight times magnification. The inferior limit was set in the mid-sagittal view as the most inferior transverse plane perpendicular to the rostral-most point of the genu of the corpus callosum. The caudal limit was the genu of the corpus callosum. The superior limit was defined as 10 axial slices (inclusive) superior to the inferior limit.

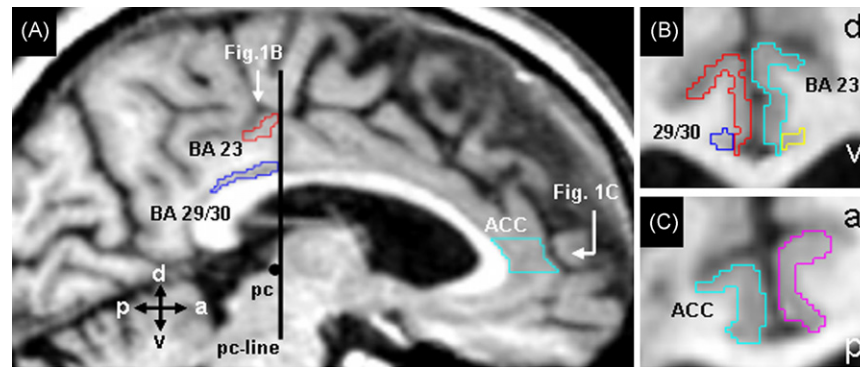


Fig. 1. Cingulate regions of interest. (A) Sagittal section of MRI scan (left hemisphere) indicating the sampled ROIs of the cingulate gyrus. (B) Coronal section demonstrating posterior cingulate gyrus subdivisions (left and right BA 23 and BA 29/30). (C) Axial section demonstrating the sampled anterior cingulate cortex (BA 24 and 33). Note the 20 mm cortical ribbon length for BA 23 and ACC. Key: a, anterior; ACC, anterior cingulate cortex; d, dorsal; p, posterior; pc, posterior commissure; v, ventral.

The rostral limit was set at 20 mm of cortical ribbon length as described for BA 23 (Fig. 1C). Effectively, the pre-genual ACC was sampled (BA 24 and 33).

2.4.3. Total intracranial volume (TIV) estimation

Based on the results of a previous methodological study of TIV estimation methods (Pengas et al., *in press*), the mid-cranial PD method was used to estimate TIV. This involved manually tracing the intracranial boundary for each subject in 10 contiguous axial supratentorial slices and multiplying by the slice thickness.

2.5. Reproducibility

A repeat measurement of each region of interest (ROI) was performed for the first 10 subjects, at least 1 week after the original measurements. Two methods of assessing intra-rater reliability for each method were used.

2.5.1. Coefficient of variation (CV)

This was calculated as $CV = (\text{standard deviation of the ROI differences between two time points} / \text{mean of the ROI differences between two time points}) \times 100\%$ (Rudick et al., 1999).

2.5.2. Mean absolute percentage difference (MAPD)

This was calculated as the absolute difference between two measurements of the ROI divided by the average ROI volume of the two measurements, multiplied by 100%.

2.6. Statistical analysis

2.6.1. Matching for TIV

The analysis of covariance method described for normalisation of ROIs using TIV (Jack et al., 1989), was used to correct all volumes. All subsequent analyses were performed based on volumes corrected for TIV.

2.6.2. Atrophy in incipient AD

Unpaired two-tailed Student's *t*-tests were performed between groups for each ROI volume. To further characterise the extent of atrophy in each region, the percentage reduction in volume compared to controls was estimated as $\% \text{ atrophy}_i = ((\text{mean control volume}_i - \text{mean patient volume}_i) / \text{mean control volume}_i) \times 100\%$, where *i* is the same ROI. In addition, the degree of correlation between atrophic regional volumes in patients was assessed using Pearson's product-moment correlation coefficients.

Given that hippocampal atrophy is an established finding in incipient AD, our main aim was to determine whether BA 29/30 and BA 23 atrophy, if present, was comparable to the amount of hippocampal volume loss. As shown in Table 4, however, the raw volumes of the ROIs, were not of comparable size. Volumes for each ROI were therefore converted to *z*-scores relative to the control mean. Furthermore, because the central issue was how BA 29/30 and BA 23 compared to the hippocampus, and not any hemispheric differences, a mean for each ROI pair (right and left hippocampus, right and left BA 29/30, etc.) was taken to limit the number of statistical tests. These scores were then entered as a within-subjects factor into a two-way repeated-measures ANOVA with group entered as a between-subjects factor, using Sidak for correction of multiple pairwise comparisons. Planned *a priori* comparisons to test the following null hypotheses were carried out in the patient group: (a) that the ACC (negative control) was not significantly different from the hippocampus (positive control), BA 23 and BA 29/30 and (b) that the hippocampus (positive control) was not significantly different from BA 23 and BA 29/30.

2.6.3. Age of onset

It has been proposed that posterior cingulate involvement is more significant in early-onset AD (Shiino et al., 2006), whereas the hippocampus is more affected in late-onset AD (Kemp et al., 2003; Frisoni et al., 2005). To address this question of differential involvement of the posterior cingulate

Table 2
Demographics by age group

	Early-onset AD	Late-onset AD	Young controls	Old controls
Gender (M:F)	4:6	5:9	8:6	9:5
Years to AD diagnosis from symptom onset (σ)	5.9 (3.5)	5.3 (1.8)	–	–
Age at symptom onset (range)	57.8 (53–63)	70.5 (66–77)	–	–
Age at scan (range)	61.7 (57–65)	73.5 (69–80)	58.1 (50–64)	71.7 (66–83)
MMSE at scan (σ)	26.9 (1.4)	26.8 (1.4)	29.6 (0.7)	29.0 (0.9)

cortex and the hippocampus with respect to age of onset, Pearson's correlation coefficients were calculated for the mean (left and right hemisphere) corrected volumes and age of onset in patients and age in controls.

Furthermore, to examine the specific hypothesis that patients with onset before age 65 show more severe posterior cingulate atrophy than late-onset patients (Shiino et al., 2006), we subdivided our patient group into early- (age at onset ≤ 65 , $n = 10$) and late-onset (age at onset > 65 , $n = 14$) subgroups. The control group was also subdivided into young and old subjects with the same age criteria (see Table 2). Z-Scores were then recalculated based on the age-matched control subgroups and differences between the two age subgroups were examined by unpaired Student's *t*-tests for each ROI. The use of *z*-scores in this way, is, in effect, comparing the difference in standard deviations between the patient mean and the control (aged matched) mean.

3. Results

3.1. Reproducibility

The reproducibility results are summarised in Table 3.

3.2. Focal atrophy in incipient AD

The raw and TIV corrected volumes are presented in Table 4. Between group comparisons (unpaired Student's *t*-tests) of volumes corrected for TIV show significant reduction in patients vs. controls in the hippocampus, BA 29/30 and BA 23 ($p < 0.001$ in all). There was no significant atrophy in the ACC. Furthermore, significant *percentage* volume reductions were found in the hippocampus (19.4%), BA 29/30 (19.4%) and BA 23 (18.2%) (Fig. 2). It can be seen that the amount of atrophy is very similar between the hippocampus and posterior cingulate regions.

The results of the pairwise correlations of atrophic regions (hippocampus, BA 29/30 and BA 23) in patients are presented in Table 5.

The two-way repeated-measures ANOVA of the mean regional (left and right hemisphere) *z*-scores found a statistically significant group-by-region interaction ($F(3,150) = 14$, $p < 0.001$). This means that the regions, as expected, showed different profiles in patients and controls, and therefore planned comparisons of regions were carried out only in patients.

Pairwise comparisons, in patients, with the hippocampus as the reference region, showed that there was no significant difference in the magnitude of volume loss between the hippocampal and BA 29/30 *z*-scores (mean difference hippocampus – BA 29/30: $z = -0.45$, $p > 0.3$), nor between the hippocampal and BA 23 *z*-scores (mean difference hippocampus – BA 23: $z = -0.07$, $p > 0.9$). There was a significant difference between the hippocampal and anterior cingulate *z*-scores (mean difference hippocampus – ACC: $z = -1.83$, $p < 0.001$) (Fig. 3). Furthermore, the null hypothesis that there is no difference in atrophy between the ACC and the other three regions was rejected ($F(1,23) = 58.1$, $p < 0.001$), while the null hypothesis of no difference in atrophy between the hippocampus and BA 23 and BA 29/30 was not refuted ($F(1,23) = 0.97$, $p > 0.3$).

3.3. The effect of age of onset

The TIV corrected volumes per ROI in early- and late-onset patients and young and old controls are presented in Table 6. The results of correlations of TIV corrected volumes with age of onset for each ROI in patients and controls are presented in Table 7. These analyses showed a significant negative correlation between the hippocampal volume and increasing age in patients and healthy controls. BA 23 was negatively correlated to age in controls.

Unpaired Student's *t*-tests, comparing early- with late-onset patient groups by region, using *z*-scores derived from

Table 3
Reproducibility data

	Hippocampus		BA 29/30		BA 23		ACC		TIV
	Rt	Lt	Rt	Lt	Rt	Lt	Rt	Lt	
CV (%)	1.83	3.17	4.82	4.30	4.35	3.50	2.33	2.27	0.21
MAPD (%)	2.68	5.44	7.48	5.16	7.70	6.25	4.44	3.92	0.40

Key: CV, coefficient of variance; MAPD, mean absolute percentage difference; ACC, anterior cingulate cortex; TIV, total intracranial volume.

Table 4
ROI volumes

Region	Incipient AD	Controls
Raw volumes		
Hippocampus	1308 (302)	1690 (304)
BA 29/30	180 (54)	228 (59)
BA 23	424 (76)	514 (83)
ACC	530 (75)	498 (58)
TIV corrected volumes		
Hippocampus	1340 (318)	1663 (266)
BA 29/30	182 (53)	226 (58)
BA 23	422 (77)	516 (82)
ACC	531 (74)	496 (57)

Key: all values are mean volumes in mm³ (standard deviation).

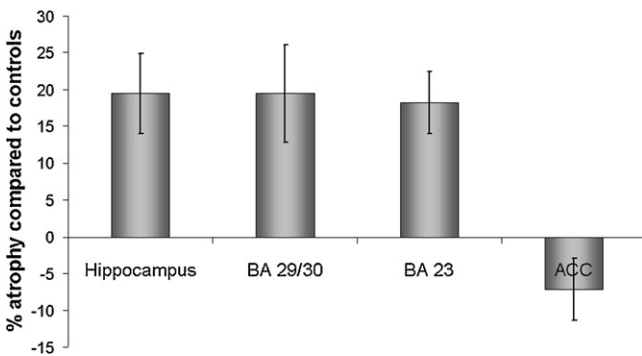


Fig. 2. Percentage volume loss in incipient AD vs. controls. Key: Rt, right; Lt, left, BA 29/30, Brodmann area 29/30; BA23, Brodmann area 23; ACC, anterior cingulate cortex; HC, hippocampus; *, unpaired *t*-test $p < 0.05$. Error bars represent the 95%CI.

Table 5
Correlations between atrophic regional volumes in patients

Comparison	<i>p</i>	<i>R</i>	<i>R</i> ²	Slope
HC vs. BA 29/30	0.2	0.19	0.04	0.03
HC vs. BA 23	0.86	0.03	0.001	0.06
BA 29/30 vs. BA 23	0.001*	0.46	0.21	0.67

Key: HC, hippocampus, *significant ($p < 0.05$).

age-matched control subgroups, revealed no significant differences for the hippocampus, BA 23 or ACC (see Fig. 4). There was a significant difference between early- and late-onset AD patients for BA 29/30 ($p < 0.01$) but this showed that late-onset patients had more atrophy in BA 29/30 than early-onset patients.

4. Discussion

To our knowledge, this is the first study that has directly compared the relative atrophy of hippocampal and cingulate structures at the MCI-stage, in patients who have all subsequently fulfilled the criteria for probable (sporadic) AD. The results confirmed the prior hypothesis that posterior cingulate (BA 29/30 and BA 23) atrophy is present in incipient

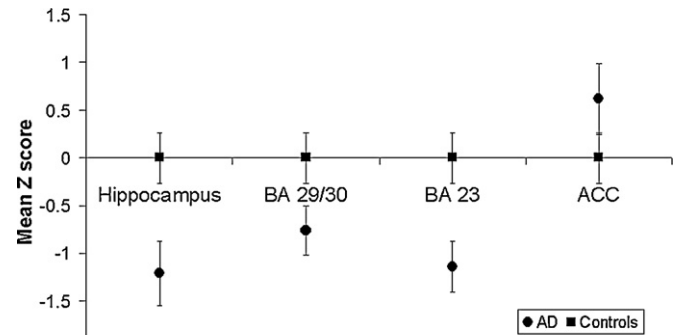


Fig. 3. Mean z-scores by region. Error bars represent the 95%CI.

AD. Furthermore, posterior cingulate atrophy was specific, in that it was found in the absence of anterior cingulate cortex atrophy, indicating that it is not merely a marker of global cortical atrophy.

The magnitude of atrophy in BA 29/30 and BA 23 was strongly correlated. This is not surprising given that these ROIs lie adjacent to each other. However, there was no significant correlation between the hippocampus and either of the two posterior cingulate ROIs, even though posterior cingulate atrophy (19% in BA 29/30 and 18% in BA 23) was as marked as that of the hippocampus (19%). Taken together, these results suggest that, although by symptom onset, both parts of the limbic system have atrophied to a similar degree in incipient AD, the two areas are not necessarily degenerating in concert in individual patients.

A pathological study of BA 23 in control subjects showed that neurodegeneration was not present over four decades of normal aging (Vogt et al., 1998); in contrast, patients with confirmed AD ($n = 72$), showed five qualitatively different laminar patterns of BA 23 neurodegeneration. Importantly, each pattern was present early in the disease and was independent of disease duration (disease duration range 1–25 years) (Vogt et al., 1998), although no cognitive data were supplied. The present results indicate that posterior cingulate degeneration is already established when AD patients are only at the MCI stage. This finding, in a substantial sporadic cohort, is concordant with MRI results in four pre-symptomatic subjects that were gene positive for autosomal dominant AD (Scahill et al., 2002). Using a fluid-registration technique on longitudinal MRI data, the study found that only two sites (the hippocampus and the posterior cingulate) were subject to accelerated atrophy before symptom onset.

Previous volumetric MRI studies have reported posterior cingulate cortex atrophy in *established* AD. Jones et al. (2006) studied ten patients with familial AD at an advanced stage (mean MMSE 10.5) and found 44% atrophy in BA 23 and 22% atrophy in BA 29/30. Similarly, Barnes et al. (2007) reported increased rates of atrophy in the posterior cingulate (and hippocampus) in 19 patients (mean MMSE = 20). Both of these studies, however, also found anterior cingulate atrophy. One study (Callen et al., 2001), found posterior cingulate and hippocampal atrophy (effect sizes 1.12 and 1.77, respec-

Table 6
TIV corrected volumes and percentage atrophy by ROI according to age of onset

	Hippocampus	BA 29/30	BA 23	ACC
Incipient AD				
Early-onset: volume	1448 (246)	202 (55)	447 (52)	542 (66)
Early-onset: % reduction	14.4	9.0	15.3	−6.7
Late-onset: volume	1262 (344)	168 (48)	404 (88)	524 (81)
Late-onset: % reduction	22.7	27.0	19.7	−8.3
Controls				
Young: volume	1692 (255)	222 (58)	528 (66)	508 (71)
Old: volume	1633 (279)	230 (58)	503 (96)	484 (36)

Key: all values are means, volumes are in mm³ (standard deviation).

Table 7
Correlations with age of onset using corrected volumes

	<i>p</i>	<i>R</i>	<i>R</i> ²	Slope
Controls				
Hippocampus vs. age at scan	0.03*	0.29	0.08	−0.01
BA 29/30 vs. age at scan	0.9	0.01	0	0
BA 23 vs. age at scan	0.02*	0.31	0.1	−0.05
ACC vs. age at scan	0.23	0.16	0.03	−0.02
Incipient AD				
Hippocampus vs. age at onset	0.01*	0.36	0.13	−0.008
BA 29/30 vs. age at onset	0.16	0.21	0.04	−0.03
BA 23 vs. age at onset	0.72	0.05	0	0
ACC vs. age at onset	0.83	0.03	0	0

Key: *significant correlation *p* < 0.05.

tively) in the absence of anterior cingulate atrophy, but as all the subjects had established AD (mean MMSE = 19.5), it was impossible to know whether posterior cingulate involvement was an early, or a later, feature.

VBM studies in MCI have reported mixed results with respect to the posterior cingulate. Some found posterior cingulate volume loss in the absence of anterior cingulate

changes (Chetelat et al., 2002; Karas et al., 2004; Shiino et al., 2006), others found combined posterior and anterior cingulate atrophy (Bozzali et al., 2006), while some reported no posterior cingulate changes (Chetelat et al., 2005; Pennanen et al., 2005). Some of this inconsistency probably relates to diagnostic uncertainty and heterogeneity in cases designated MCI—not all studies included longitudinal outcome (Chetelat et al., 2002; Karas et al., 2004; Pennanen et al., 2005) and, of those that did report findings for patients that subsequently “converted” to AD, numbers were very small for VBM (Chetelat et al., 2005; Bozzali et al., 2006; Shiino et al., 2006). Finally, some directly contrasted cases designated “converters” and “non-converters” (Chetelat et al., 2005; Bozzali et al., 2006). This approach introduces the potential confound that a “non-converter” group might harbour AD cases that have been followed-up for an insufficient period to establish their true fate.

In common with this study’s design, one recent VBM study did specifically focus on MCI cases (*n* = 33) that all subsequently progressed to fulfil probable AD criteria (Whitwell et al., 2007). The authors found bilateral hippocampal, but not posterior cingulate involvement both at baseline and at the probable AD stage and speculated that this may have been because their cases were over 65 years old. This hypothesis is based on earlier studies using ^{99m}Tc-HMPAO single photon emission computed tomography (Kemp et al., 2003) and VBM (Ishii et al., 2005; Shiino et al., 2006) which suggested that posterior cingulate involvement was specifically associated with onset of AD before 65 years. The present study directly addressed this hypothesis and found no supportive evidence for differential posterior cingulate and hippocampal atrophy according to age of onset. Consistent with earlier findings (Jack et al., 1997b) there was a significant negative correlation between hippocampal volumes and age in patients and healthy controls. The same correlation was found for BA 23 in healthy controls. There was, however, no evidence for greater posterior cingulate atrophy in early-onset AD when subgroups (early- and late-onset) were contrasted with age-matched control subgroups. In fact, if anything, there was evidence that the magnitude of atrophy in BA 29/30 was greater in late-onset disease. Failure to demonstrate an association between early-onset AD and disproportionate posterior cingulate atrophy is consistent with evidence from FDG-PET

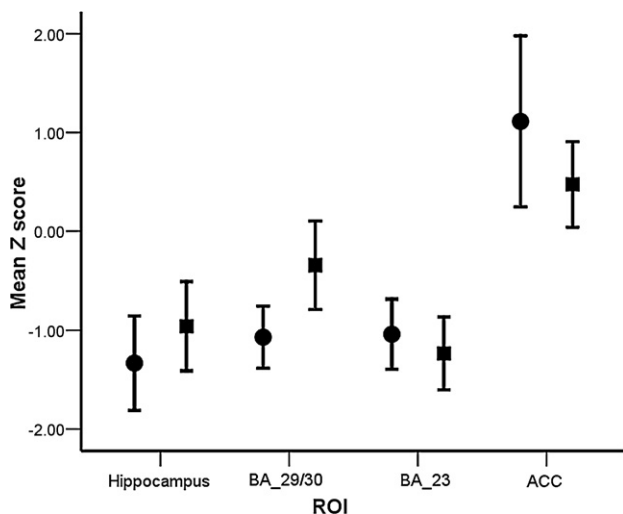


Fig. 4. Age of onset analysis. Mean z-scores by region in patients with incipient AD, subdivided into late- (circles) and early-onset (squares) subgroups. Late- and early-onset AD z-scores were calculated based on age-matched control subgroups. Error bars represent the 95%CI.

(Grady et al., 1987) and neuropathology (Armstrong et al., 2000) that also failed to find these age-related subtypes.

Despite the present study's design advantages over some VBM reports for studying incipient AD, certain limitations warrant mention. BA 29/30 is a particularly small structure with quite large inter-individual variability (volume range: 137–412 mm³, standard deviation: 61 mm³ in controls). All measurements were performed by a single rater and therefore only intra-rater reliability could be assessed. Assessing inter-rater reliability would be an important aspect of future work. Only the rostral parts of BA 23 and BA 29/30 were sampled, even though voxel-based analyses suggest that the posterior cingulate gyrus slightly caudal to this ROI is the area of maximal damage, both in terms of hypometabolism (Nestor et al., 2003) and atrophy (Scahill et al., 2002). This could mean that the area of most significant posterior cingulate atrophy was not sampled. Although this may have underestimated the magnitude of regional atrophy, the present protocol was preferred in order to maintain consistent landmarks and enhance reproducibility.

It is possible that posterior cingulate degeneration is a contributor to the clinical phenotype in AD. Patients with isolated retrosplenial lesions have relatively pure topographical disorientation: they can recognise landmarks, yet they cannot orient using them; they do not know which direction to take and are unable to find their way in familiar environments or learn new routes. These deficits arise in the context of intact MTLs, e.g. Takahashi et al. (1997); for a review see Maguire (2001). In addition, anterograde and retrograde episodic amnesia secondary to a relatively isolated retrosplenial cortex lesion, termed "retrosplenial amnesia" (Valenstein et al., 1987), has been reported. AD patients most prominently suffer from episodic amnesia and they almost universally develop topographical disorientation as the disease progresses (Monacelli et al., 2003). The relevance of the present study findings, of focal posterior cingulate atrophy in incipient AD, to the cognitive profile of the earliest presentation of the disease is an important subject for further research.

In conclusion, this study found significant atrophy in the posterior cingulate (BA 23 and BA 29/30) in incipient AD, comparable to that found in the hippocampus. Sparing of the ACC highlights that this finding is not simply a consequence of global cortical atrophy. Furthermore, the results are consistent with the prior hypothesis that focal posterior cingulate hypometabolism, previously demonstrated in incipient AD, may, to a significant degree, be a consequence of local pathology. Nevertheless, these findings do not exclude the possibility that de-afferentation from the MTL may also contribute to posterior cingulate hypometabolism. It is unclear why the MTL and posterior cingulate are selectively vulnerable in AD. Interestingly, in the posterior cingulate, the atrophy involves archicortex (BA 29/30) and adjacent isocortex (BA 23). This is analogous to the MTL, where archicortex (hippocampus) and adjacent isocortex (parahippocampal gyrus) are both atrophic. Whether the observation that posterior cin-

gulate, and hippocampal, atrophy are comparable in incipient disease can shed light on the neurobiology of AD, remains to be seen.

Conflicts of interest

None.

Acknowledgements

We gratefully acknowledge our patients and their relatives for participating in research studies. PJN, PW and JRH are funded by the Medical Research Council (UK). GP is funded by the Alzheimer's Research Trust (UK).

References

- Alladi, S., Arnold, R., Mitchell, J., Nestor, P.J., Hodges, J.R., 2006. Mild cognitive impairment: applicability of research criteria in a memory clinic and characterization of cognitive profile. *Psychol. Med.* 36 (4), 507–515.
- Armstrong, R.A., Nochlin, D., Bird, T.D., 2000. Neuropathological heterogeneity in Alzheimer's disease: a study of 80 cases using principal components analysis. *Neuropathology* 20 (1), 31–37.
- Barnes, J., Godbolt, A.K., Frost, C., Boyes, R.G., Jones, B.F., Scahill, R.I., Rossor, M.N., Fox, N.C., 2007. Atrophy rates of the cingulate gyrus and hippocampus in AD and FTLD. *Neurobiol. Aging* 28 (1), 20–28.
- Bozzali, M., Filippi, M., Magnani, G., Cercignani, M., Franceschi, M., Schiatti, E., Castiglioni, S., Mossini, R., Falautano, M., Scotti, G., Comi, G., Falini, A., 2006. The contribution of voxel-based morphometry in staging patients with mild cognitive impairment. *Neurology* 67 (3), 453–460.
- Braak, H., Braak, E., 1991. Neuropathological staging of Alzheimer-related changes. *Acta Neuropathol.* 82 (4), 239–259.
- Callen, D.J., Black, S.E., Gao, F., Caldwell, C.B., Szalai, J.P., 2001. Beyond the hippocampus: MRI volumetry confirms widespread limbic atrophy in AD. *Neurology* 57 (9), 1669–1674.
- Chan, D., Fox, N.C., Scahill, R.I., Crum, W.R., Whitwell, J.L., Leschziner, G., Rossor, A.M., Stevens, J.M., Cipolotti, L., Rossor, M.N., 2001. Patterns of temporal lobe atrophy in semantic dementia and Alzheimer's disease. *Ann. Neurol.* 49 (4), 433–442.
- Chetelat, G., Desgranges, B., De La Sayette, V., Viader, F., Eustache, F., Baron, J.C., 2002. Mapping gray matter loss with voxel-based morphometry in mild cognitive impairment. *Neuroreport* 13 (15), 1939–1943.
- Chetelat, G., Landeau, B., Eustache, F., Mezenge, F., Viader, F., de la Sayette, V., Desgranges, B., Baron, J.C., 2005. Using voxel-based morphometry to map the structural changes associated with rapid conversion in MCI: a longitudinal MRI study. *Neuroimage* 27 (4), 934–946.
- De Santi, S., de Leon, M.J., Rusinek, H., Convit, A., Tarshish, C.Y., Roche, A., Tsui, W.H., Kandil, E., Boppana, M., Daisley, K., Wang, G.J., Schlyer, D., Fowler, J., 2001. Hippocampal formation glucose metabolism and volume losses in MCI and AD. *Neurobiol. Aging* 22 (4), 529–539.
- Duvernoy, H.M., 1999. *The Human Brain: Surface, Three-Dimensional Sectional Anatomy with MRI, and Blood Supply*. Wien, Springer-Verlag Wien.
- Folstein, M.F., Folstein, S.E., McHugh, P.R., 1975. "Mini-mental state". A practical method for grading the cognitive state of patients for the clinician. *J. Psychiatr. Res.* 12 (3), 189–198.
- Frisoni, G.B., Testa, C., Sabattoli, F., Beltramello, A., Soininen, H., Laakso, M.P., 2005. Structural correlates of early and late onset Alzheimer's disease: voxel based morphometric study. *J. Neurol. Neurosurg. Psychiatry* 76 (1), 112–114.

- Galton, C.J., Patterson, K., Graham, K., Lambon-Ralph, M.A., Williams, G., Antoun, N., Sahakian, B.J., Hodges, J.R., 2001. Differing patterns of temporal atrophy in Alzheimer's disease and semantic dementia. *Neurology* 57 (2), 216–225.
- Grady, C.L., Haxby, J.V., Horwitz, B., Berg, G., Rapoport, S.I., 1987. Neuropsychological and cerebral metabolic function in early vs. late onset dementia of the Alzheimer type. *Neuropsychologia* 25 (5), 807–816.
- Hasboun, D., Chantome, M., Zouaoui, A., Sahel, M., Deladoeuille, M., Sourour, N., Duyme, M., Baulac, M., Marsault, C., Dormont, D., 1996. MR determination of hippocampal volume: comparison of three methods. *AJNR Am. J. Neuroradiol.* 17 (6), 1091–1098.
- Ishii, K., Kawachi, T., Sasaki, H., Kono, A.K., Fukuda, T., Kojima, Y., Mori, E., 2005. Voxel-based morphometric comparison between early- and late-onset mild Alzheimer's disease and assessment of diagnostic performance of z score images. *AJNR Am. J. Neuroradiol.* 26 (2), 333–340.
- Jack, C.R., Petersen, R.C., Xu, Y.C., Waring, S.C., O'Brien, P.C., Tangalos, E.G., Smith, G.E., Ivnik, R.J., Kokmen, E., 1997a. Medial temporal atrophy on MRI in normal aging and very mild Alzheimer's disease. *Neurology* 49 (3), 786–794.
- Jack, C.R., Petersen, R.C., Xu, Y.C., O'Brien, P.C., Smith, G.E., Ivnik, R.J., Boeve, B.F., Waring, S.C., Tangalos, E.G., Kokmen, E., 1999. Prediction of AD with MRI-based hippocampal volume in mild cognitive impairment. *Neurology* 52 (7), 1397–1403.
- Jack Jr., C.R., Twomey, C.K., Zinsmeister, A.R., Sharbrough, F.W., Petersen, R.C., Cascino, G.D., 1989. Anterior temporal lobes and hippocampal formations: normative volumetric measurements from MR images in young adults. *Radiology* 172 (2), 549–554.
- Jack Jr., C.R., Petersen, R.C., Xu, Y.C., Waring, S.C., O'Brien, P.C., Tangalos, E.G., Smith, G.E., Ivnik, R.J., Kokmen, E., 1997b. Medial temporal atrophy on MRI in normal aging and very mild Alzheimer's disease. *Neurology* 49 (3), 786–794.
- Jones, B.F., Barnes, J., Uylings, H.B., Fox, N.C., Frost, C., Witter, M.P., Scheltens, P., 2006. Differential regional atrophy of the cingulate gyrus in Alzheimer disease: a volumetric MRI study. *Cereb. Cortex*.
- Karas, G.B., Scheltens, P., Rombouts, S.A., Visser, P.J., van Schijndel, R.A., Fox, N.C., Barkhof, F., 2004. Global and local gray matter loss in mild cognitive impairment and Alzheimer's disease. *Neuroimage* 23 (2), 708–716.
- Kemp, P.M., Holmes, C., Hoffmann, S.M., Bolt, L., Holmes, R., Rowden, J., Fleming, J.S., 2003. Alzheimer's disease: differences in technetium-99m HMPAO SPECT scan findings between early onset and late onset dementia. *J. Neurol. Neurosurg. Psychiatry* 74 (6), 715–719.
- Maguire, E.A., 2001. The retrosplenial contribution to human navigation: a review of lesion and neuroimaging findings. *Scand. J. Psychol.* 42 (3), 225–238.
- Mathuranath, P.S., Nestor, P.J., Berrios, G.E., Rakowicz, W., Hodges, J.R., 2000. A brief cognitive test battery to differentiate Alzheimer's disease and frontotemporal dementia. *Neurology* 55 (11), 1613–1620.
- McKhann, G., Drachman, D., Folstein, M., Katzman, R., Price, D., Stadlan, E.M., 1984. Clinical diagnosis of Alzheimer's disease: report of the NINCDS-ADRDA Work Group under the auspices of Department of Health and Human Services Task Force on Alzheimer's disease. *Neurology* 34 (7), 939–944.
- Minoshima, S., Giordani, B., Berent, S., Frey, K.A., Foster, N.L., Kuhl, D.E., 1997. Metabolic reduction in the posterior cingulate cortex in very early Alzheimer's disease. *Ann. Neurol.* 42 (1), 85–94.
- Monacelli, A.M., Cushman, L.A., Kavcic, V., Duffy, C.J., 2003. Spatial disorientation in Alzheimer's disease: the remembrance of things passed. *Neurology* 61 (11), 1491–1497.
- Morris, J.C., 1993. The Clinical Dementia Rating (CDR): current version and scoring rules. *Neurology* 43 (11), 2412–2414.
- Nagahama, Y., Okina, T., Suzuki, N., Matsuda, M., 2006. The Cambridge behavioral inventory: validation and application in a memory clinic. *J. Geriatr. Psychiatry Neurol.* 19 (4), 220–225.
- Nestor, P.J., Fryer, T.D., Smielewski, P., Hodges, J.R., 2003. Limbic hypometabolism in Alzheimer's disease and mild cognitive impairment. *Ann. Neurol.* 54 (3), 343–351.
- Nestor, P.J., Fryer, T.D., Hodges, J.R., 2006. Declarative memory impairments in Alzheimer's disease and semantic dementia. *Neuroimage* 30 (3), 1010–1020.
- Pengas, G., Pereira, J.M.S., Williams, G.B., Nestor, P.J., in press. Comparative reliability of total intracranial volume estimation methods and the effect of atrophy in a longitudinal semantic dementia cohort. *J. Neuroimag.*
- Pennanen, C., Testa, C., Laakso, M.P., Hallikainen, M., Helkala, E.L., Hanninen, T., Kivipelto, M., Kononen, M., Nissinen, A., Tervo, S., Vanhanen, M., Vanninen, R., Frisoni, G.B., Soininen, H., 2005. A voxel based morphometry study on mild cognitive impairment. *J. Neurol. Neurosurg. Psychiatry* 76 (1), 11–14.
- Rudick, R.A., Fisher, E., Lee, J.C., Simon, J., Jacobs, L., 1999. Use of the brain parenchymal fraction to measure whole brain atrophy in relapsing-remitting MS. Multiple Sclerosis Collaborative Research Group. *Neurology* 53 (8), 1698–1704.
- Scahill, R.I., Schott, J.M., Stevens, J.M., Rossor, M.N., Fox, N.C., 2002. Mapping the evolution of regional atrophy in Alzheimer's disease: unbiased analysis of fluid-registered serial MRI. *Proc. Natl. Acad. Sci. U.S.A.* 99 (7), 4703–4707.
- Shiino, A., Watanabe, T., Maeda, K., Kotani, E., Akiguchi, I., Matsuda, M., 2006. Four subgroups of Alzheimer's disease based on patterns of atrophy using VBM and a unique pattern for early onset disease. *Neuroimage* 33 (1), 17–26.
- Takahashi, N., Kawamura, M., Shiota, J., Kasahata, N., Hirayama, K., 1997. Pure topographic disorientation due to right retrosplenial lesion. *Neurology* 49 (2), 464–469.
- Valenstein, E., Bowers, D., Verfaellie, M., Heilman, K.M., Day, A., Watson, R.T., 1987. Retrosplenial amnesia. *Brain* 110 (Pt 6), 1631–1646.
- Vogt, B.A., Nimchinsky, E.A., Vogt, L.J., Hof, P.R., 1995. Human cingulate cortex: surface features, flat maps, and cytoarchitecture. *J. Comp. Neurol.* 359 (3), 490–506.
- Vogt, B.A., Vogt, L.J., Vrana, K.E., Gioia, L., Meadows, R.S., Challa, V.R., Hof, P.R., Van Hoesen, G.W., 1998. Multivariate analysis of laminar patterns of neurodegeneration in posterior cingulate cortex in Alzheimer's disease. *Exp. Neurol.* 153 (1), 8–22.
- Vogt, B.A., Vogt, L.J., Perl, D.P., Hof, P.R., 2001. Cytology of human caudomedial cingulate, retrosplenial, and caudal parahippocampal cortices. *J. Comp. Neurol.* 438 (3), 353–376.
- Wahlund, L.O., Julin, P., Johansson, S.E., Scheltens, P., 2000. Visual rating and volumetry of the medial temporal lobe on magnetic resonance imaging in dementia: a comparative study. *J. Neurol. Neurosurg. Psychiatry* 69 (5), 630–635.
- Watson, C., Jack Jr., C.R., Cendes, F., 1997. Volumetric magnetic resonance imaging. Clinical applications and contributions to the understanding of temporal lobe epilepsy. *Arch. Neurol.* 54 (12), 1521–1531.
- Whitwell, J.L., Przybelski, S.A., Weigand, S.D., Knopman, D.S., Boeve, B.F., Petersen, R.C., Jack Jr., C.R., 2007. 3D maps from multiple MRI illustrate changing atrophy patterns as subjects progress from mild cognitive impairment to Alzheimer's disease. *Brain* 130 (Pt 7), 1777–1786.
- Zola-Morgan, S., Squire, L.R., Amaral, D.G., 1986. Human amnesia and the medial temporal region: enduring memory impairment following a bilateral lesion limited to field CA1 of the hippocampus. *J. Neurosci.* 6 (10), 2950–2967.